

# Preparation, Structure and Properties of Nitrile–Butadiene Rubber–Organoclay Nanocomposites by Reactive Mixing Intercalation Method

Lan Liu, Demin Jia, Yuanfang Luo, Baochun Guo

College of Materials Science and Engineering, South China University of Technology, Guangzhou 510640, China

Received 22 February 2005; accepted 8 August 2005

DOI 10.1002/app.22614

Published online 2 February 2006 in Wiley InterScience (www.interscience.wiley.com).

**ABSTRACT:** The nanocomposites of nitrile–butadiene rubber (NBR) and organo-montmorillonite modified by hexadecyltrimethyl ammonium bromide (HMMT) were prepared by the reactive mixing intercalation method in the presence of the resorcinol and hexamethylenetetramine complex (RH). The structure of the NBR–RH–HMMT nanocomposites was characterized by XRD, TEM, FTIR, determination of crosslinking density, and so on. The results showed that the *d*-spacing of HMMT increased substantially with RH addition and the layers of HMMT were dispersed in rubber matrix on a nanometer scale. The mechanical

properties of the NBR–RH–HMMT nanocomposites were far superior to those of NBR–HMMT composites, and the glass transition temperature of NBR–RH–HMMT nanocomposite was higher than that of NBR. The reactive mixing intercalation method by introducing RH could enhance the interface combination between the rubber and the organoclay through the interactions of RH with NBR and modified clay. © 2006 Wiley Periodicals, Inc. *J Appl Polym Sci* 100: 1905–1913, 2006

**Key words:** nitrile–butadiene rubber; montmorillonite; nanocomposites

## INTRODUCTION

Rubber–clay nanocomposites are a new class of composites that have unique mechanical, thermal, and barrier properties. Generally, there are two main processes to prepare rubber–clay nanocomposites. In one case, the monomer is intercalated and then polymerized *in situ* in the interlayer galleries of clay. The other method is the direct intercalation of polymers in solution, latex, or melt state.<sup>1–8</sup> Solution intercalation method needs a compatible rubber–solvent system and modified organoclay. Its disadvantages are the environment pollution caused by the solvents and the difficulty of removing the solvents. Latex intercalation needs co-coagulation of the rubber latex and clay suspension and then drying of the mixture. The procedure is complicated. Compared with the latex and solution intercalation method, the mechanically mixing intercalation method is a convenient way and easy-to-realize industrialization. It is an applicable approach to produce the rubber-based nanocomposites and can be applied in most of rubbers. In general, however, only some segments of rubber macromolecules can intercalate into the interlayer galleries of the

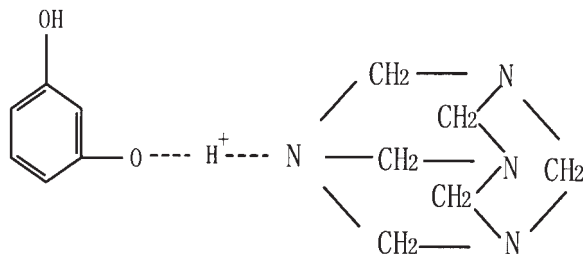
clay by mixing intercalation method since rubber is a high molecular weight polymer with very high viscosity in the processing state and has very poor interfacial adhesion with the layers of clay.

In our previous work,<sup>9,10</sup> a new method for preparing the rubber–clay nanocomposites by introducing some monomers into natural rubber (NR) latex/organoclay system was investigated. During the process of emulsion polymerization, the monomer could graft onto NR macromolecules and, at the same time, intercalate into the galleries of clay and polymerize *in situ*. This method can enhance the interfacial adhesion between the inorganic layers and the rubber matrix so that the mechanical properties of NR–organoclay nanocomposites were greatly improved. However, this latex intercalation needs to polymerize the monomer and then co-coagulate the rubber latex and organoclay. The procedure is still complicated.

In this study, the authors attempt to develop a new kind of preparation method for rubber–clay nanocomposites, called as reactive mixing intercalation method, by introducing some reactive monomers in rubber mixing and vulcanization process. Nitrile–butadiene rubber (NBR) was adopted in the experiments. The organoclay (HMMT) was prepared by ion exchanging Na<sup>+</sup>-montmorillonite with hexadecyl-trimethylammonium bromide. The monomers adopted resorcinol and hexamethylenetetramine complex (RH, the structural formula is shown in Scheme 1). RH is an usual adhesive in rubber industry, which can be de-

Correspondence to: L. Liu (psliulan@scut.edu.cn).

Contract grant sponsor: The Natural Science Foundation of China; contract grant number: 59933060.



**Scheme 1** Structural formula of RH.

composed into resorcinol and formaldehyde at the temperature above 110°C and can react with NBR in the process of vulcanization.<sup>11</sup> New kinds of nanocomposites, NBR–RH–HMMT nanocomposites, were prepared by reactive mixing intercalation method and the structure and properties of the nanocomposites were studied.

## EXPERIMENTAL

### Materials

NBR (N41, acrylonitrile content 29%) was purchased from Japan Synthetic Rubber Co. (Tokyo, Japan); Organoclay HMMT was supplied from our laboratory; RH is of industrial grade; Hexadecyl-trimethylammonium bromide is chemical pure reagent. Other materials are of chemical pure grade.

### Preparation of organoclay

Organoclay HMMT was prepared by ion exchanging Na<sup>+</sup>-montmorillonite with hexadecyl-trimethylammonium bromide as follows. Na<sup>+</sup>-montmorillonite (50 g, cation exchange capacity: 119 mEq/100 g) was dispersed into 2000 mL of hot water (about 80°C) by using a homogenizer. Hexadecyl-trimethylammonium bromide was dissolved into hot water and poured into the montmorillonite–water solution under vigorous stirring for 4 h, producing a white precipitate. The precipitate was collected and washed with hot water three times, and dried to yield an organoclay.

### Preparation of NBR–RH–HMMT nanocomposites

NBR, HMMT, RH, and other ingredients were mixed by a Φ 160 mm open two-roll mill by a standard procedure. Then, the compound was cured in a compression mold at the temperature of 160°C. The formulations of the compounds are shown in Table I. The vulcanizates are referred to as NBR–RH–HMMT nanocomposites.

### Characterization and testing

An X-ray diffraction (XRD) measurement on the power was performed using the D/MAX-III power diffractometer equipped with Cu Kα radiation ( $\lambda = 1.54 \text{ \AA}$ ).

Transmitted electron microscopy (TEM) observations were performed with a JEOL JEM-100SX microscope using an acceleration voltage of 80 kV. The samples were prepared by using an ultramicrotome in a liquid nitrogen trap.

Fourier transform infrared (FTIR) spectra of powder samples were recorded using a Nicolet Migana 760 FTIR spectrometer at a resolution of 4 cm<sup>-1</sup> in the absorbance mode.

Crosslink density was determined by equilibrium swelling method. The samples were swollen in acetone at room temperature to an equilibrium state and then removed from the solvent, and the acetone on the surface was quickly blotted off with tissue paper. The samples were immediately weighed on an analytical balance to the tolerance of 1 mg and then dried at vacuum. Assuming the mass loss of the rubber during swelling is the same for all the samples, the volume fraction of rubber in swollen gel ( $V_r$ ), which was used to represent the crosslinking density of the vulcanizates, was determined by the following equation:

$$V_r = \frac{1}{1 + \left(\frac{m_b}{m_a} - 1\right) \times \frac{\rho_r}{\alpha \rho_s}}$$

Where  $m_a$  and  $m_b$  is the sample masses before and after swelling,  $\rho_r$  and  $\rho_s$  is the density of rubber and solvent, respectively,  $\alpha$  is the mass fraction of rubber in the vulcanizates.

Tensile and tear testing were performed on sample cut from 1 mm thick sheet and tested using a Shimadzu AG-1 electron tensile tester according to ISO/DIS37–1990 and ISO034–1979 respectively. Shore A hardness was measured according to ISO7619–1986.

**TABLE I**  
Formulations of the Compounds of NBR and Its Composites

Compounds	A	B	C	D
NBR	100	100	100	100
HMMT	0	10	10	10
RH	0	0	4	8
Zinc oxide	4	4	4	4
Stearic acid	2	2	2	2
Accelerator CZ	1.5	1.5	1.5	1.5
Accelerator DM	0.5	0.5	0.5	0.5
Antioxidant 4010NA	1.5	1.5	1.5	1.5
Unsolvable sulfur	1.5	1.5	1.5	1.5

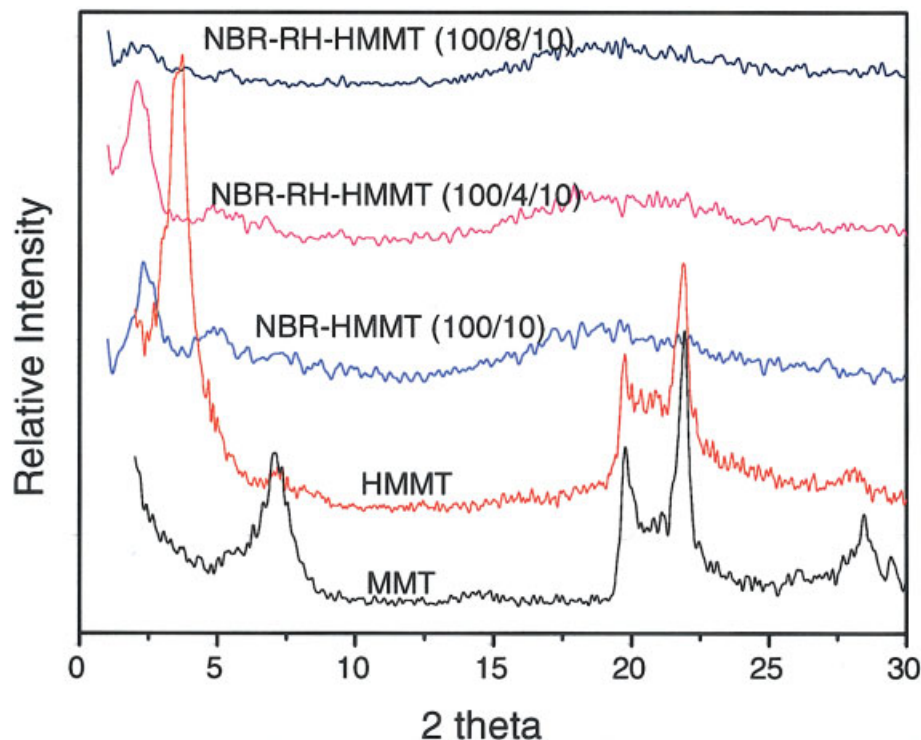


**Figure 1** The XRD patterns of MMT, HMMT, and the composites. [Color figure can be viewed in the online issue, which is available at [www.interscience.wiley.com](http://www.interscience.wiley.com)]

A TA Instruments Universal V1.7F DMA2980 instrument was used for dynamic mechanical analysis (DMA) in the tension mode on a sample with approximate 6 mm width and 1.5 mm height. Temperature scans from  $-120$  to  $200^{\circ}\text{C}$  were carried out at a rate of  $3^{\circ}\text{C}/\text{min}$  and frequency of 10 Hz.

## RESULTS AND DISCUSSION

### XRD results of clay and its nanocomposites

Figure 1 shows the XRD patterns of MMT, HMMT, NBR-HMMT (100/10), NBR-RH-HMMT (100/4/10), and NBR-RH-HMMT (100/8/10), respectively, and the interlayer spacings ( $d_{001}$  values) in MMT, HMMT, and the nanocomposites calculated according to Bragg equation are shown in Table II. MMT shows a charac-

teristic diffraction peak (001 diffraction peak) around  $2\theta = 6.90^{\circ}$ ; the corresponding interlayer spacing is 1.3 nm. The organomontmorillonite HMMT presents a peak around  $3.34^{\circ}$ ; the corresponding interlayer spacing is 2.6 nm. It is suggested that the interlayers of HMMT are successfully intercalated by organic modifier and its interlayer galleries are obviously expanded. The  $d$ -spacing of NBR-HMMT nanocomposite is expanded to 3.9 nm due to the organic modification of the clay providing a hydrophobic environment for the intragallery adsorption of the polymer, which improves the interfacial properties between the polymer and inorganic phases. The  $d_{001}$  values of NBR-RH-HMMT nanocomposites were further increased to 4.2 nm and 4.8 nm when RH content is 4 phr and 8 phr, respectively, indicating that RH facilitates the intercalation of macromolecular segments into the interlayer galleries of clay through the reaction of RH with NBR and HMMT during the processes of mixing and vulcanization.

**TABLE II**  
The Interlayer Spacings ( $d_{001}$ ) in Clay and Its Nanocomposites

Sample	HMMT content (phr)	RH content (phr)	$2\theta$ ( $^{\circ}$ )	$d_{001}$ (nm)
MMT	—	—	6.90	1.3
HMMT	—	—	3.34	2.6
NBR-HMMT	10	—	2.24	3.9
NBR-RH-HMMT	10	4	2.05	4.2
NBR-RH-HMMT	10	8	1.80	4.8

### Morphology of NBR-organoclay nanocomposites

Figure 2 is the TEM photographs of NBR-HMMT and NBR-RH-HMMT nanocomposites. The dark lines in the photos correspond to the intersections of the silicate layer. It is apparent that in Figure 2(a) the dispersion of the layered silicate in NBR-HMMT composite is not uniform. There are the particles with thickness

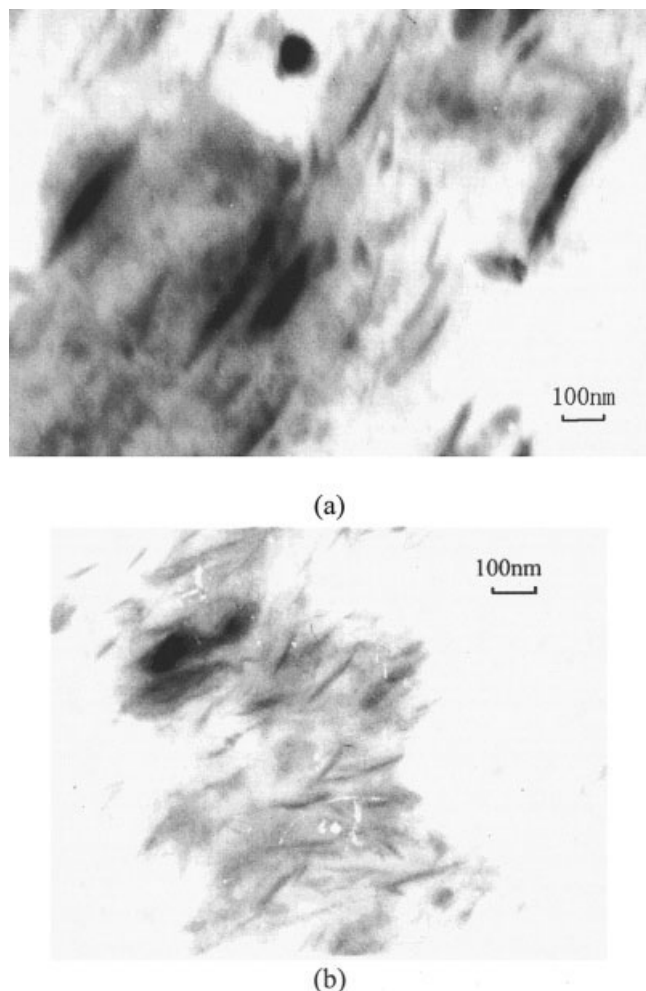


**Figure 2** TEM photographs of (a) NBR-HMMT (100/10) and (b) NBR-RH-HMMT (100/8/10) nanocomposites.

of about 10–50 nm and the aggregates with sizes of more than 100 nm. Figure 2(b) shows that the layered silicate is further divided into thinner bundles with thickness of 5–20 nm and lengths of about 100 nm dispersed uniformly in rubber matrix, and there are still individual larger aggregates with sizes of more than 50 nm. Therefore it could be considered that the preparation of NBR-RH-HMMT nanocomposites is successful due to the addition of RH. RH could improve the dispersion of HMMT in rubber matrix and the interfacial adhesion between rubber macromolecule chains and silicate layers, and hence increase the intercalation efficiency.

#### Crosslinking density and extraction ratio of NBR-RH-HMMT nanocomposites

The crosslinking densities of NBR vulcanizate and its composites are shown in Table III. It is shown that the crosslinking density of NBR-HMMT composite is higher than that of neat NBR. This suggests that the

**TABLE III**  
Crosslinking Densities of NBR Vulcanizate and Its Nanocomposites

Sample	HMMT content (phr)	RH content (phr)	$V_r$
NBR	—	—	0.28
NBR-HMMT	10	—	0.30
NBR-RH	—	4	0.32
NBR-RH	—	8	0.35
NBR-RH-HMMT	10	4	0.34
NBR-RH-HMMT	10	8	0.39

NBR became more crosslinked in the presence of the organoclay owing to the chain segments of NBR intercalated into the galleries of silicate and facilitated the crosslink formation. The addition of RH in NBR-RH-HMMT nanocomposites further increases the crosslinking densities of the vulcanizates. This may be attributed to the chemical crosslinking by phenol-formaldehyde and physical crosslinking by the HMMT layers. The mechanism will be discussed later.

The extraction ratios of the vulcanizate of NBR and its composites by acetone are shown in Table IV. It is shown that the extraction ratio of NBR-HMMT is lower than that of neat NBR. The addition of RH in NBR-RH-HMMT further decreases the extraction ratio of the composites. The decreased extraction ratio may be due to the chemical crosslinking effects of phenol-formaldehyde on NBR and the confinement of the intercalated NBR chains by the silicate layers. This is consistent with the results of the crosslinking density.

#### Mechanical properties of NBR-RH-HMMT nanocomposites

Table V presents the results of the mechanical properties of the NBR vulcanizate and its composites. Compared with the neat NBR, the mechanical properties of NBR-HMMT nanocomposites increase dramatically. By adding RH, the mechanical properties of NBR-RH-HMMT nanocomposites are further improved at 300% modulus, tensile strength, tear strength, and elongation at break. The reinforcing ef-

**TABLE IV**  
Extraction Ratios of the Vulcanizates of NBR and Its Composites by Acetone

Sample	HMMT content (phr)	RH content (phr)	Ex (%)
NBR	—	—	9.38
NBR-HMMT	10	—	5.23
NBR-RH-HMMT	10	4	3.31
NBR-RH-HMMT	10	8	2.77

TABLE V  
Mechanical Properties of NBR (A), NBR-HMMT (B), and NBR-RH-HMMT (C, D) Vulcanizates

	A	B	C (100/4/10)	D (100/8/10)
Modulus at 300% (MPa)	2.23	4.65	6.22	6.94
Tensile strength (MPa)	2.77	13.76	15.41	16.84
Elongation at break (%)	460	630	640	660
Permanent set (%)	6	14	16	18
Tear strength (KN/m)	10.40	22.15	26.34	30.45
Hardness (shore A)	50	54	54	58
After ageing in air (100±1°C, 48h)				
Modulus at 300% (MPa)	1.58	3.47	6.69	7.72
Tensile strength (MPa)	2.06	9.83	12.36	14.24
Elongation at break (%)	260	450	500	540
Permanent set (%)	4	8	10	12
Tear strength (KN/m)	8.05	17.36	22.75	26.62
Hardness (shore A)	54	60	60	62
Property descend ratio <sup>a</sup> (%)	58.0	49.0	37.3	30.8

<sup>a</sup> Property descend ratio =  $\{[(\text{tensile strength} \times \text{elongation at break})_{\text{before aging}} - (\text{tensile strength} \times \text{elongation at break})_{\text{after aging}}] / (\text{tensile strength} \times \text{elongation at break})_{\text{before aging}}\} \times 100\%$ .

iciency can be assigned to the dispersion of silicates in NBR matrix at nanometer level and the increasing in the crosslinking density by the reaction of RH with NBR and HMMT during the processes of mixing and vulcanization, which improve the interface properties and facilitate the macromolecular intercalating into silicate layers. Furthermore, the results of ageing test demonstrate that the mechanical properties of NBR-RH-HMMT nanocomposites after ageing in air for 48 h at (100 ± 1)°C are better than those of NBR-HMMT nanocomposites. The results suggested that the high aspect ratio characteristic of silicate layers in nanocomposites and the reaction of RH in matrix could not only reinforce the rubber but also increase the crosslinking density and enhance the interfacial adhesion between the NBR and silicate layers, which could improve the aging resistance of the system.

#### DMA analysis of NBR-RH-HMMT nanocomposites

DMA for NBR-RH-HMMT nanocomposites were carried out to monitor the layers of organoclay and the effect of RH on the thermodynamic properties of NBR nanocomposites. The storage modulus ( $G'$ ), loss modulus ( $G''$ ) and loss factor ( $\tan \delta$ ) are plotted in Figure 3. It can be seen that the NBR-RH-HMMT (100/8/10) nanocomposite has higher  $G'$  value than that of NBR-HMMT and pure NBR over the whole temperature range (Fig. 3(a)). The trend can be attributed to the higher crosslink density and better dispersion of the nanolayers with the effect of RH. The loss modulus and loss factors of NBR, NBR-HMMT, and NBR-RH-HMMT nanocomposites also can be observed in Figure 3(b) and 3(c), respectively. The loss moduli of them have the same trend as that of dynamic relax-

ation. The  $T_g$ s and the  $\tan \delta$  values at 0°C and 60°C are summarized in Table VI. The  $T_g$  of NBR-HMMT increases from -14.5°C for pure NBR to -11.6°C. This may be due to the existence of the interaction between nanolayers of organoclay and NBR matrix, which confinement of the motion of the macromolecular chains segments. The  $\tan \delta$  peak of NBR-RH-HMMT nanocomposites gradually shifted to a slightly higher temperature in comparison to NBR-HMMT nanocomposites and NBR. The  $T_g$  of NBR-RH-HMMT nanocomposites further increase to -9.8°C and -7.3°C when RH content is 4 phr to 8 phr, respectively. The results indicate that in the NBR-RH-HMMT nanocomposites, the mobility of NBR chains is further restricted by the reaction products of RH with NBR and HMMT, giving rise to increase the  $T_g$  of nanocomposites. As shown in Table VI, the  $\tan \delta$  value of NBR-RH-HMMT nanocomposites is higher at 0°C and lower at 60°C owing to the shift of relaxation peak to the higher temperature in virtue of higher crosslinking density under the reaction of RH. It is indicated that the nanocomposites have better damping property around room temperature and lower heat build-up at higher temperature.

#### Formation mechanism of NBR-RH-HMMT nanocomposites

It is well known that RH can be decomposed into resorcinol and formaldehyde at the temperature above 110°C. To research the intercalation of RH into the layers of HMMT, the mixture of HMMT and resorcinol (RF), the decomposition product of RH, was mixed at 110°C and analyzed by XRD. Figure 4 shows the XRD patterns of (a) HMMT and (b) HMMT/RF and Table VII summarizes the interlayer spacings

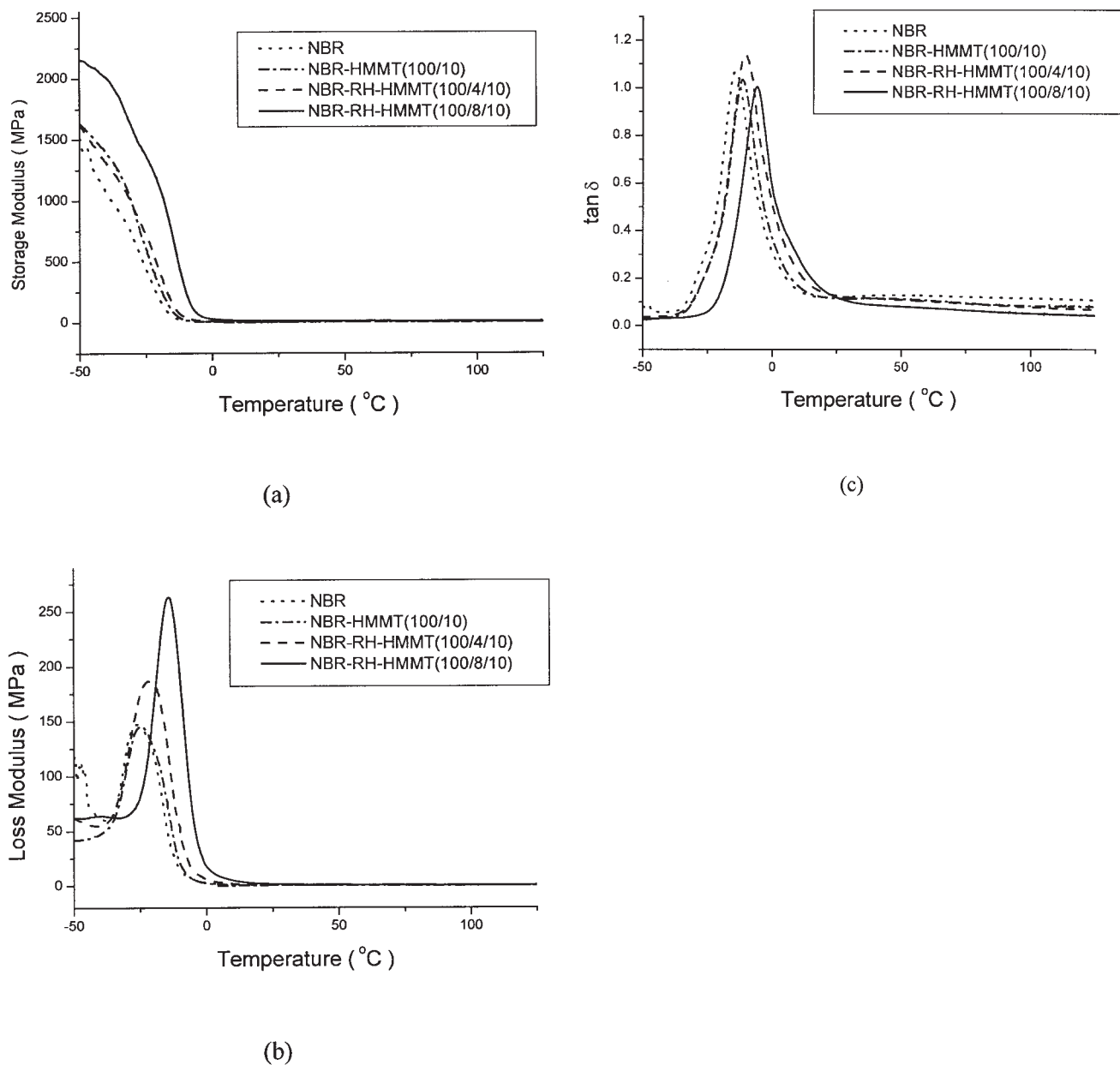


**Figure 3** The curves of dynamic mechanical properties for NBR, NBR-HMMT, and NBR-RH-HMMT nanocomposites.

( $d_{001}$ ) of HMMT and HMMT/RF. It is obvious that the  $d_{001}$  peak of HMMT/RF moves forward and the  $d_{001}$  value increases from 2.58 nm of HMMT to 3.31 nm of

HMMT/RF. It suggests that RF could intercalate into HMMT galleries in the process of vulcanization.

To substantiate the reactions between RH and NBR, FTIR analysis of NBR-RH-HMMT composite during heating at 160°C was performed. The results are shown in Figure 5. The absorbance of the band at 760  $\text{cm}^{-1}$ , characterizing the disubstituted benzene, decreases gradually while that of the band at 835  $\text{cm}^{-1}$ , characterizing the tetrasubstituted benzene, increases gradually during heating. This indicates the formation of phenol-formaldehyde by the condensation polymerization between resorcinol and formaldehyde during vulcanization. In addition, the absorbance at 1620  $\text{cm}^{-1}$  decreases during heating, indicating that the

**TABLE VI**  
The  $T_g$  and  $\tan \delta$  Values of NBR and Its Composites from DMA

	$T_g$ (°C)	$\tan \delta$ (0°C)	$\tan \delta$ (60°C)
NBR	-14.5	0.3107	0.1263
NBR-HMMT (100/10)	-11.6	0.3651	0.1068
NBR-RH-HMMT (100/4/10)	-9.8	0.5132	0.1029
NBR-RH-HMMT (100/8/10)	-7.3	0.6405	0.0744

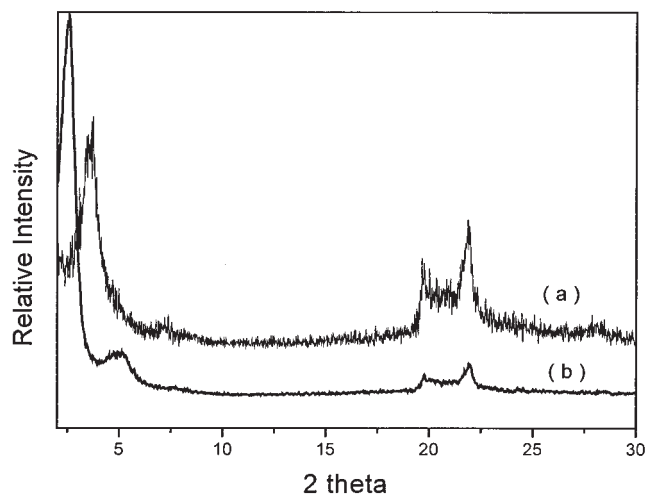


Figure 4 XRD patterns of (a)HMMT and (b) HMMT/RF.

addition reactions of the C=C double bonds on the NBR chains take place.

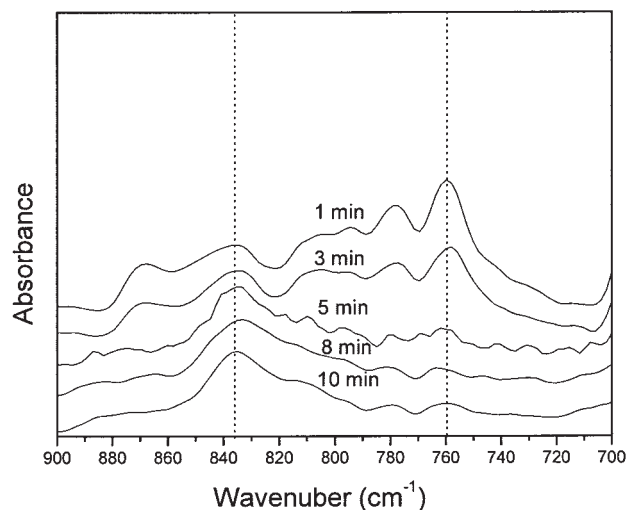
According to the above results, the authors proposed the following reaction mechanisms between RH and NBR and between RH and HMMT. As shown in Scheme 2(a), resorcinol and formaldehyde obtained from the decomposition of RH polymerize and crosslink to form phenol-formaldehyde resin. At the same time, NBR reacts with the phenol-formaldehyde by addition reaction of double bonds in butadiene or by substitution reaction of  $\alpha$ -hydrogen atoms of butadiene in NBR, as shown in Scheme 2(b). The phenol-formaldehyde resin formed by the intercalation and polymerization *in situ* of RH in the interlayer galleries of HMMT may be connected with HMMT layers through the hydrogen bonds between the hydroxyl groups on the surfaces of HMMT layers and those of the phenol-formaldehyde resin, as illustrated in Scheme 2(c). Consequently, these interactions may improve the interfacial combination between the NBR and HMMT and promote the silicate layers dispersed in rubber matrix on a nanometer level.

### CONCLUSIONS

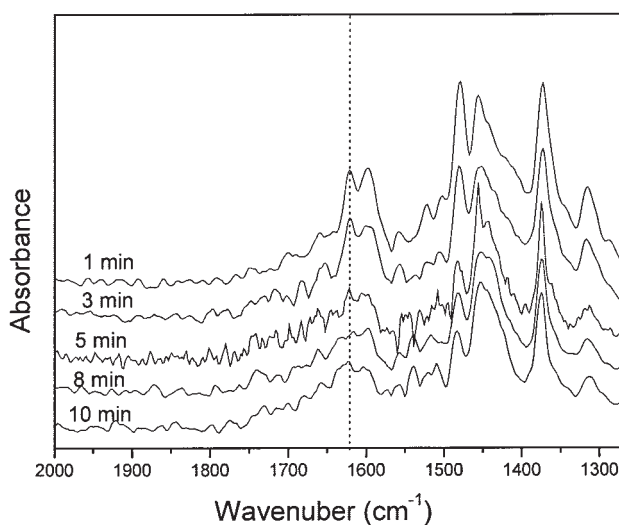
The nanocomposites of NBR and HMMT could be prepared by the mechanically reactive mixing intercalation method with RH. The  $d$ -spacing of HMMT in

TABLE VII  
The Interlayer Spacings ( $d_{001}$ ) of HMMT and HMMT/RF

Sample	HMMT	HMMT/RF
$d_{001}$ (nm)	2.58	3.31



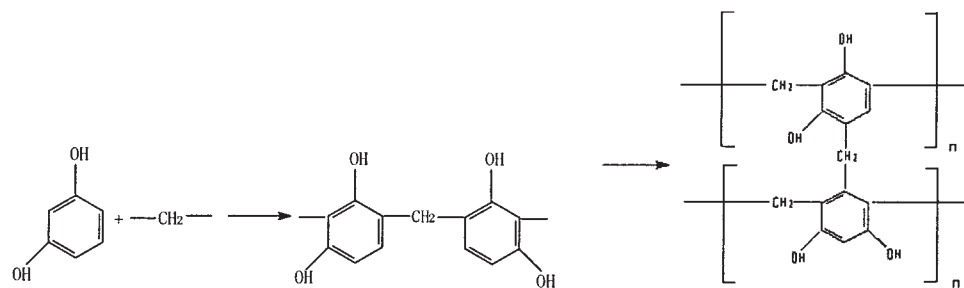
(a)



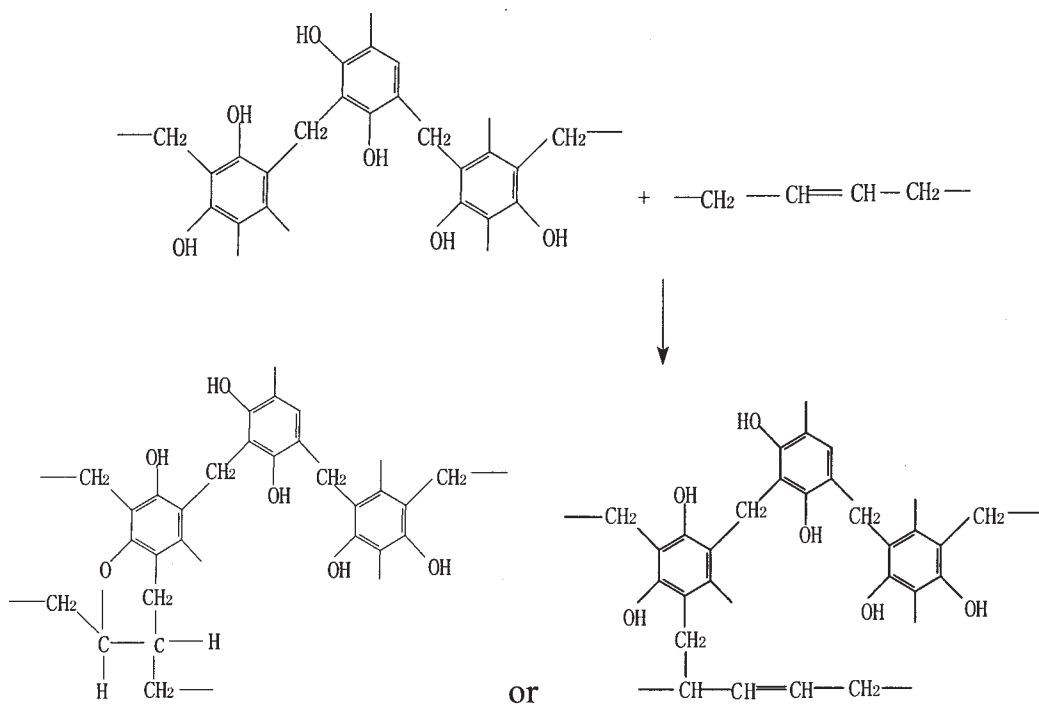
(b)

Figure 5 FTIR evolution of NBR-RH-HMMT composites during heating at 160°C.

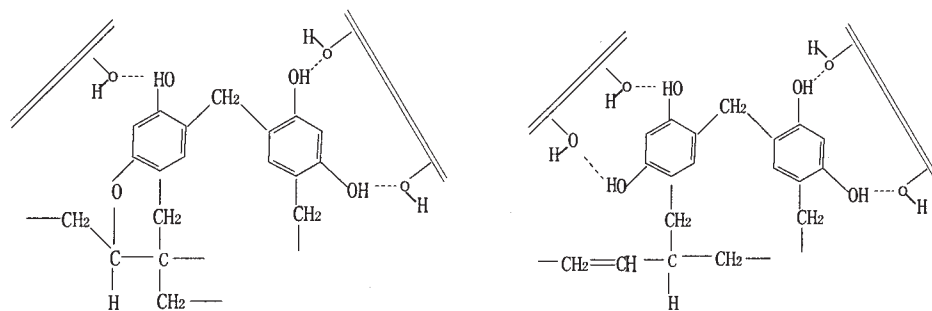
the nanocomposites increased substantially with RH addition and the layers of HMMT were dispersed in rubber matrix on a nanometer scale. The mechanical properties of the NBR-RH-HMMT nanocomposites were far superior to those of corresponding NBR-HMMT composites and NBR vulcanizate, and the  $T_g$  of NBR-RH-HMMT nanocomposite was higher than that of NBR. The reactive mixing intercalation method by introducing RH could enhance the interface combination between the rubber and the organoclay through the interactions of RH with NBR and organoclay.



(a)



(b)



(c)

**Scheme 2** Reaction mechanism between RH and NBR with HMMT.



**References**

1. Sadhu, S.; Bhowmick, A. K. *Rubber Chem Technol* 2003, 76, 860.
2. You, C. J.; Jia, D. M.; Zhen, Z. Y.; Ding, K.; Xi, S.; Mo, H. L.; Zhang, Y. H. *Chinese J Polym Sci* 2003, 21, 551.
3. Kim, J. T.; Oh, T. S.; Lee, D. H. *Polym Int* 2003, 52, 1058.
4. Pramanik, M.; Srivastava, S. K.; Samantaray, B. K.; Bhowmick, A. K. *J Appl Polym Sci* 2003, 87, 2216.
5. Nah, C.; Ryu, H. J.; Han, S. H.; Rhee, J. M.; Lee, M. H. *Polym Int* 2001, 50, 1265.
6. Nah, C.; Ryu, H. J.; Kim, W. D.; Chang, Y. W. *Polym Int* 2003, 52, 1359.
7. Wang, S. J.; Long, C. F.; Wang, X. Y.; Li, Q.; Qi, Z. N. *J Appl Polym Sci* 1998, 69, 1557.
8. Wu, Y. P.; Zhang, L. Q.; Wang, Y. Q.; Liang, Y.; Yu, D. S. *J Appl Polym Sci* 2001, 82, 2842.
9. Liu, L.; Luo, Y. F.; Zhang, F.; Huang, M. Y.; Jia, D. M. *Chin Synth Rubber Ind* 2002, 25, 262.
10. Jia, D. M.; Luo, Y. F.; Liu, L.; Zheng, Z. Y. *Chin. Pat. CN 1,397,572A* (2002).
11. Jain, R.; Nando, G. B. *Rubber World* 1988, 199, 40.